IEEE Access
Multidisciplinary ⋮ Rapid Review ⋮ Open Access Journal

Received November 9, 2021, accepted November 18, 2021, date of publication December 6, 2021,
date of current version December 23, 2021.

*Digital Object Identifier 10.1109/ACCESS.2021.3133390*

# Q-Band LEO Earth Observation Data Downlink: Radiowave Propagation and System Performance

**FELIX CUERVO[1], JOHANNES EBERT[1], MICHAEL SCHMIDT[1], (Member, IEEE), AND PANTELIS-DANIEL ARAPOGLOU[2], (Member, IEEE)**

[1]JOANNEUM RESEARCH, 8010 Graz, Austria
[2]ESA, European Space Research and Technology Centre, 2201 Noordwijk, The Netherlands

Corresponding author: Felix Cuervo (fcuervog@gmail.com)

This work was supported by the European Space Agency (ESA) under Contract 4000129101/20/NL/CT: "Feasibility Study of Q-Band (40 GHz) Earth Observation (EO) Data Downlink Systems," through the Austrian Research Promotion Agency.

**ABSTRACT** Earth Exploration Satellite Service (EESS) systems gather data about the Earth and its natural phenomena. Frequency bands traditionally employed by high-rate telemetry to download data from the satellite to the ground station, such as the X band (8 GHz), have become crowded. Higher frequency bands allow increasing the downlink throughput, as required by current advanced, multi-frequency sensors onboard the spacecraft (S/C). Some systems are already using or planning to use K-band (26 GHz) frequencies. The next band under consideration that can offer an increase in data volume return is the Q band (40 GHz). This paper studies the radiowave propagation aspects and the end-to-end system performance of Q-band Earth observation (EO) data downlink systems. Using standard ITU-R propagation prediction models and state-of-the-art technology specifications, simulation results are given in terms of obtained data return. Different orbit altitudes, satellite platform classes, ground station locations, antenna diameters and transmission types are considered.

**INDEX TERMS** Earth exploration, LEO, Q band, radiowave propagation.

## I. INTRODUCTION

Earth Exploration Satellite Service (EESS) systems are used to gather data about the Earth and its natural phenomena [1]. These satellites use active and/or passive sensors on-board the spacecraft (S/C) to obtain data on the Earth's soil, sea, and atmosphere for the purpose of studying and monitoring the Earth's climate and environment, amongst many other related scientific applications.

Currently, the European Earth observation (EO) systems use X band to download data from the satellite to the earth station(s). Agencies around the world have been looking at other bands to increase the downlink throughput since needs have increased and some lower bands have become crowded. The K is the next band in line to provide such downlink throughput, with 1.5 GHz of bandwidth available between 25.5 and 27 GHz. Some systems are already either using or planning to use this capacity. Studies have been made for Low Earth Orbit (LEO) satellites (e.g. [2] and [3]), and particularly the EUMETSAT MetOp Second Generation (MetOp-SG) and the Meteosat Third Generation (MTG) will use K-band link frequencies [4].

Looking forward, more bandwidth will be needed in the future. The quest for the next possible frequency band has already started, because the development cycle and maturation of the relevant technology can be long. The next band in sight is the Q band, where an allocation of 3 GHz (37.5 - 40.5 GHz) is available for EESS systems on a secondary priority. To explore the potential of this band, the European Space Agency initiated a feasibility study prepared by the consortium consisting of JOANNEUM RESEARCH (Austria), the Finnish Meteorological Institute (FMI) and VTT Technical Research Centre of Finland.

Despite being allocated to EESS as a secondary service, and hence not being able to interfere or claim protection from other primary systems, the Q band may still be interesting in situations such as high latitude isolated regions, special licensing scheme by the national regulator, flexible and opportune transmission of high data volume in short time windows, etc.

This contribution concentrates, in Section I, on the radiowave propagation aspects and, in Section II, on the

The associate editor coordinating the review of this manuscript and approving it for publication was Gerardo Di Martino.


| G/S | Latitude [°] N | Longitude [°] E | Altitude [m] AMSL |
|---|---|---|---|
| Svalbard | 78.233 | 15.382 | 435 |
| Kiruna | 67.89 | 21.05 | 400 |
| Sodankylä | 67.367 | 26.632 | 210 |
| Graz | 47.085 | 15.464 | 468 |

**FIGURE 1.** G/S locations.

end-to-end system performance of Q-band EO data downlink systems. The paper ends with the conclusions and acknowledgement.

## II. RADIOWAVE PROPAGATION IN LEO EO DATA DOWNLINK SYSTEMS AT Q BAND

Radiowave propagation effects worsen when moving to higher frequencies or to lower elevation angles, as it happens in Low Earth Orbit (LEO) missions for a relevant fraction of time. Current ITU-R (International Telecommunication Union, Radiocommunication Sector) propagation prediction models [1] provide a well-accepted framework for system design. However, they address mainly propagation effects for satellites in geostationary Earth orbit (GEO) and have been tested at K, Q and V band using only propagation measurements from GEO-based campaigns (e.g. OLYMPUS, ITALSAT and Alphasat [5], [6]). Therefore, the applicability of these models, the associated uncertainty and their extension to the LEO case (in particular for fade dynamics and atmospheric channel simulators) are still under study.

In the present activity, a detailed study on Q-Band atmospheric effects was conducted for four ground station (G/S) locations: Svalbard, Kiruna, Sodankylä and Graz. The locations are detailed in Fig. 1. The high latitude G/S are selected as they typically host EO G/S because these offer the longest visibility from the orbits employed by EO satellites. Graz was selected due to the availability of propagation data. The typical concept-of-operation for EO data downlink systems so far is to download all the data in a single G/S.

The availability[1] of a satellite communications system is the percentage of time during which the system is above a minimum signal-to-noise ratio (SNR). A target availability figure corresponds to a margin to be allocated to atmospheric losses based on statistical assumptions.

[1]In non-GEO systems, the reference period for the link availability is the period of visibility of the spacecraft during its pass over a G/S.

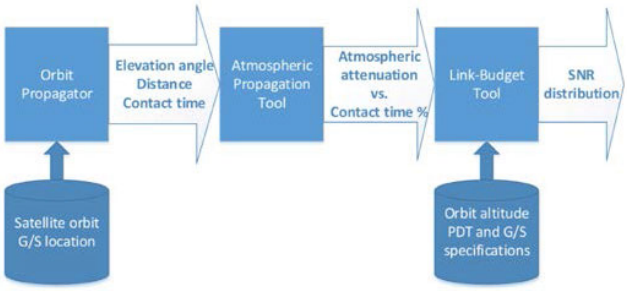


**FIGURE 2.** Block diagram of the EO data downlink receiver SNR computation.

The link budget calculator developed in the activity was used to evaluate the sensitivity to the relevant parameters (i.e. effective isotropic radiated power (EIRP), free-space loss (FSL), atmospheric attenuation, antenna gain-to-noise-temperature (G/T), etc.). The block diagram of the EO data downlink receiver SNR computation is shown in Fig. 2.

The total attenuation is an integral parameter of the link budget that depends on the radio link frequency and the distribution of the atmospheric components along the signal path: Oxygen, water vapour, clouds and precipitation. The latter, highly variable in time and space. At higher frequencies, the attenuation is higher and more variable with respect to the climatology and link elevation angle.

The contact time, elevation angle distributions and the attenuation predictions were computed for each LEO satellite orbit and G/S.

### A. LEO ORBIT

When comparing LEO orbits between 500 and 800 km altitude, differences of up to 4 dB can be observed in the FSL at Q band (40 GHz). The analysis in this paper was carried out considering three existing EO satellites with Sun-synchronous orbits (SSO) (TerraSAR-X, Sentinel-1A and NOAA-20). In Table 1, the contact time statistics are computed over an orbit repeat cycle for each orbit and G/S location. Pointing angles time series (azimuth and elevation) were computed using the satellite Two-Line Elements (TLE). Examples are shown in Fig. 3.

As shown in Table 1, the average contact times for the selected orbits and G/S range from 7 to 11 min. The elevation angle distributions (not included here), show a clear predominance of low elevation angles, with 50 % of the contact time spent well below 20° in all cases. The time availability [%] represents the percentage of time during which there is contact.

### B. ATMOSPHERIC PROPAGATION

The ITU-R Recommendation P.618-13 [7] "Propagation data and prediction methods required for the design of Earth-space telecommunication systems" contains, in section 2.5, the model for the prediction of total attenuation statistics for frequencies above 18 GHz.

**TABLE 1.** Contact time statistics for each orbit altitude and G/S location, computed for an orbit repeat cycle.

| Orbit | G/S | Orbits with contact per repeat cycle | Average contact time [min] | Total contact time per repeat cycle [min] | Time availability [%] |
|---|---|---|---|---|---|
| **TerraSAR-X** Altitude = 514 km Inclination = 97.44 ° Repeat cycle = 11 days (167 orbits) | **Svalbard** | 143 | 7.72 | 1116 | 7 |
| | **Kiruna** | 113 | 7.3 | 834 | 5.2 |
| | **Sodankylä** | 112 | 7.21 | 817.3 | 5.1 |
| | **Graz** | 51 | 7.2 | 371.5 | 2.3 |
| **Sentinel-1A** Altitude = 693 km Inclination = 98.18 ° Repeat cycle = 12 days (176 orbits) | **Svalbard** | 175 | 9.41 | 1661 | 9.6 |
| | **Kiruna** | 126 | 9.57 | 1216 | 7 |
| | **Sodankylä** | 125 | 9.53 | 1201.2 | 6.9 |
| | **Graz** | 65 | 8.9 | 583.9 | 3.3 |
| **NOAA-20** Altitude = 824 km Inclination = 98.7 ° Repeat cycle = 20 days (284 orbits) | **Svalbard** | 284 | 11.02 | 3153 | 10.9 |
| | **Kiruna** | 212 | 10.92 | 2333.1 | 8.1 |
| | **Sodankylä** | 210 | 10.91 | 2308 | 8 |
| | **Graz** | 115 | 10.1 | 1171.5 | 4 |

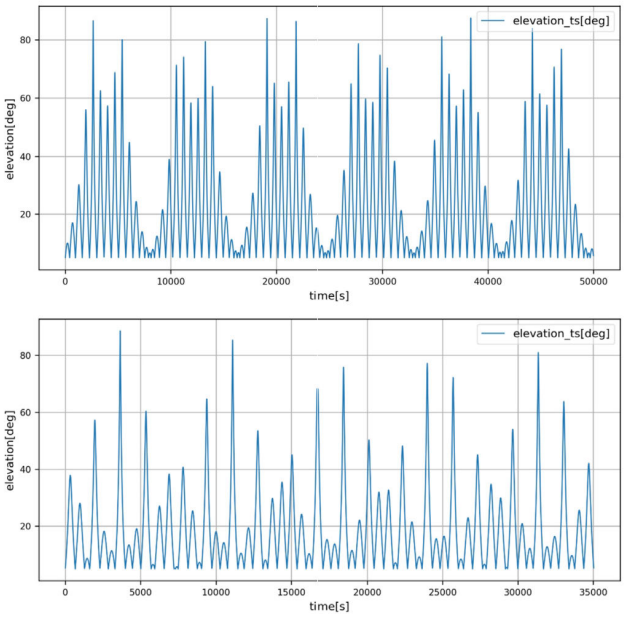


**FIGURE 3.** Orbit-cycle elevation time series (Sentinel-1A, just passes). Top: Svalbard. Bottom: Graz.

The total atmospheric attenuation is the sum of attenuation by multiple sources. The model is dependent on a number of other ITU-R Recommendations used to predict the attenuation exceeded during a certain percentage of time, which are:

- Total attenuation in ITU-R P.618-13
  - Rain attenuation in ITU-R P.618-13
    - Rain height in ITU-R P.839-4
    - Rain intensity in ITU-R P.837-7
    - Specific rain attenuation in ITU-R P.838-3
  - Cloud attenuation in ITU-R P.840-8
  - Gaseous attenuation in ITU-R P.676-12
    - Integrated water vapour content in ITU-R P.836-6
  - Scintillation in ITU-R P.618-13

In the present study, the models are run for 36 elevation angle bins from 0 to 90°. Fig. 4 shows plots of atmospheric attenuation vs. elevation angle for two selected availability percentages (95 % and 99.5 %) for the four G/S locations (with 6.8 m antenna). Also shown in the figures are vertical lines that mark the Variable Coding and Modulation (VCM) elevation sectors, as will be explained in the following sections. Note that for low elevation angles, significant attenuation values are observed at the higher availability, for which atmospheric mechanisms other than rain (clear sky conditions) are responsible.

For non-GEO systems, where the elevation angle is varying, the recommendation ITU-R P.618-13 [7] indicates how to calculate the link availability for a single satellite. The results for the four G/S locations according to the Sentinel-1A orbit are summarized in Table 2.

The different G/S locations have a big impact in the atmospheric attenuation due to the local weather and elevation angles. As expected, polar areas, which have the greater contact time, have also much better propagation conditions due to their climatic characteristics (i.e. colder and drier air).

## III. END-TO-END SYSTEM PERFORMANCE ASSESSMENT

The objective is to transmit data from the EO sensors on a LEO S/C to a single G/S. In Q band, successful transmission cannot be guaranteed in all cases due to the highly variable atmospheric attenuation. We assume in this analysis that no retransmission mechanism is used, such that data which cannot be successfully received are lost.

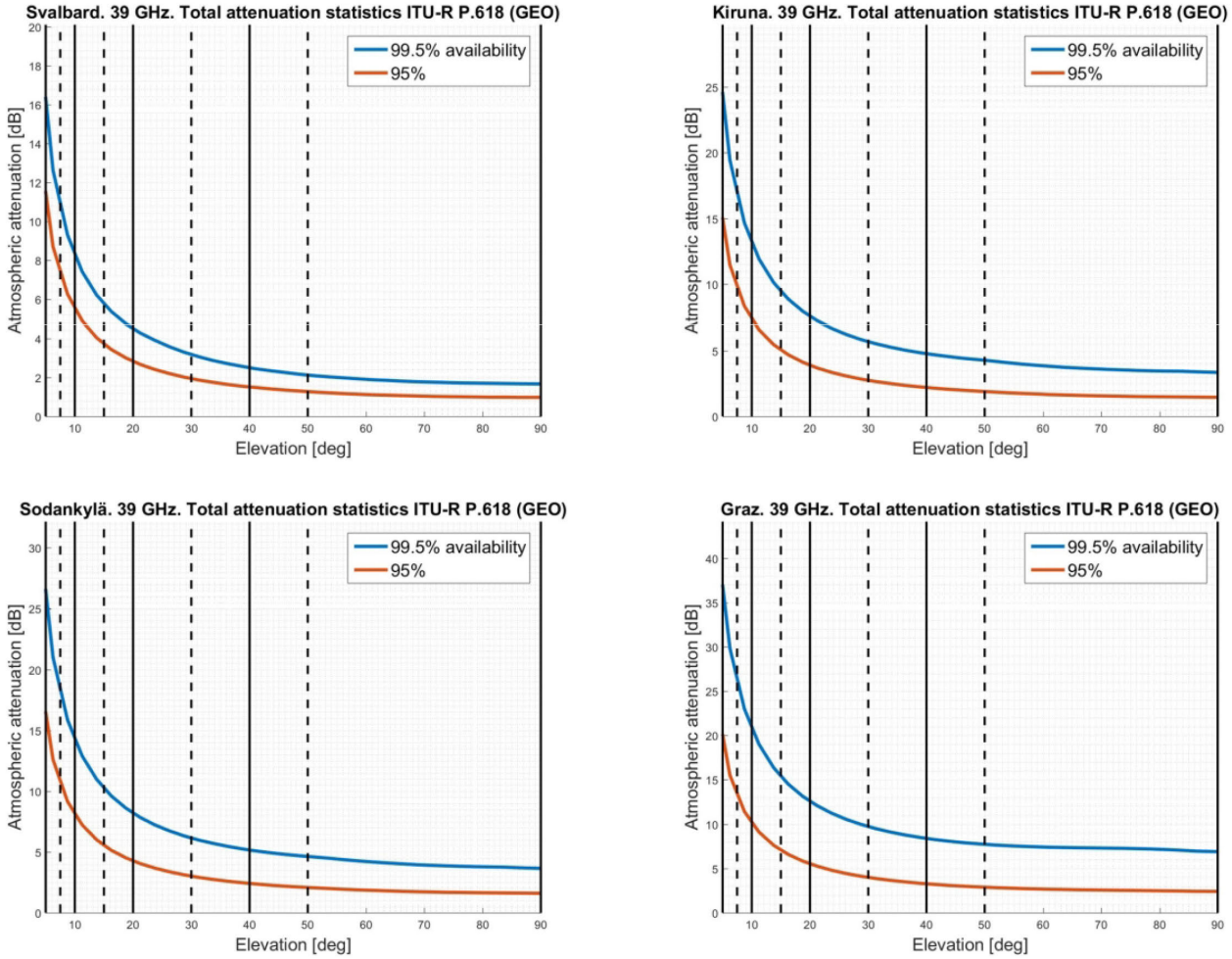


**FIGURE 4.** Total attenuation statistics at the G/S locations computed with the model in ITU-R P.618-13. VCM elevation sectors delimited with black lines (solid: 4 sectors, dashed: 8 sectors).

**TABLE 2.** Atmospheric attenuation exceeded vs. link availability weighted over the whole LEO pass above the G/S locations for the Sentinel-1A orbit.

| | Atmospheric attenuation exceeded [dB] | | | |
|---|---|---|---|---|
| Availability [%] | Svalbard | Kiruna | Sodankylä | Graz |
| 95 | 4.1 | 5.2 | 5.8 | 7.5 |
| 99.5 | 9.1 | 12.6 | 13.7 | 19.5 |

Instead, the goal is to achieve a certain link availability of e.g. 99.5%.

In the present study, the key performance indicator (KPI) to be optimized is the total amount of data downloaded per pass. An end-to-end performance analysis is done for so-called scenarios, consisting of fixed sets of parameters, which are summarized as follows:

1) Three S/C orbits (514, 693 and 824 km altitude).
2) Three S/C classes (K-band and Q-band $<$ 50 and $>$ 300 kg weight, with the corresponding EIRP and carrier sizes; see Table 3). A single channel has been assumed for all configurations with different symbol rates. The extension to multiple channels to make use of the spectrum allocation is then straightforward. A mechanically steerable antenna is assumed on board the satellite.
3) Three G/S antenna diameters (3, 6.8 and 10 m), with corresponding G/T; see Table 4). Data on the ground antenna performance has been obtained from European and Canadian antenna manufacturers.
4) Four G/S locations (Svalbard, Kiruna, Sodankylä and Graz; with the corresponding elevation angle and attenuation statistics).
5) Three transmission types: Constant, Variable and Adaptive Coding and Modulation (CCM, VCM and ACM respectively) [10]. The state-of-the-art waveforms in Consultative Committee for Space Data Systems CCSDS 131.2-B-1 [11] are used. The standard is based on the Serial Concatenated Convolutional Coding (SCCC); and defines 27 Modulation and Coding

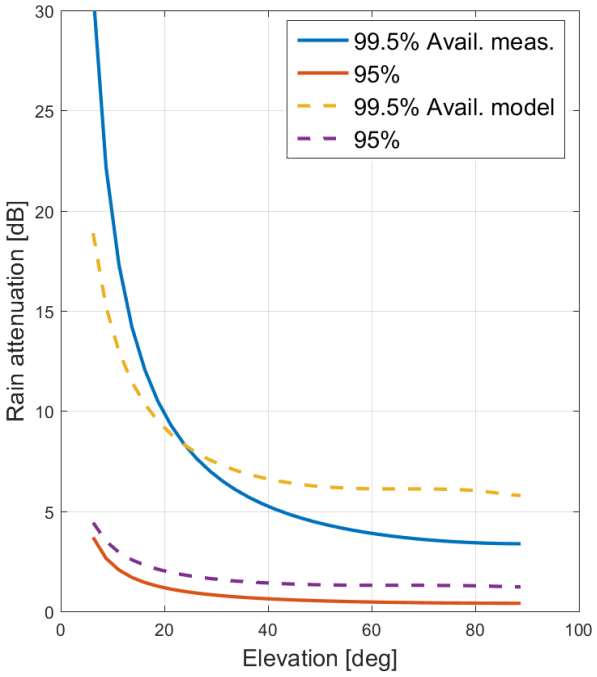


**FIGURE 5.** Graz. Alphasat (39.4 GHz) rain attenuation measured statistics scaled in elevation compared with the ITU-R P. 618-13 model predictions.

Schemes (MCS) covering a wide range of signal-to-noise ratios. The MCS selection is different for each transmission type:

- In CCM, the atmospheric attenuation with respect to the required availability at the optimal lowest elevation is taken for the calculation of the SNR and determination of the MCS. This MCS is fixed for the whole pass, and since this calculation is identical for all passes, it can be fixed for the whole orbit cycle.
- In VCM, the passes are subdivided in elevation sectors (see Fig. 4). In each of the sectors (at the low elevation bound), the atmospheric attenuation with respect to the required availability is taken for the calculation of the SNR and determination of the MCS. This MCS is fixed for each sector, and since this calculation is identical for all passes, it can be fixed for each sector during the whole orbit cycle.
- In ACM, the MCS are derived from the instantaneous SNR on the channel, measured at the ground receiver and fed back to the transmitter via an uplink channel. To compensate for the latency of the control loop and the SNR estimation errors, a 1 dB margin has been added to the MCS SNR thresholds.

The set of scenarios and their corresponding input parameter values are given in Table 5, where the baseline scenario is colored in green, and the parameter varying in each of the other scenarios is colored in yellow. The resulting KPI for 95% link availability and the performance comparison with respect to the baseline scenario are given in the columns on the right.

**TABLE 3.** S/C link budget parameters.

| Parameter | K-band | Q-band < 50 kg | Q-band > 300 kg |
|---|---|---|---|
| Frequency [GHz] | 26 | 39 | |
| EIRP [dBW] | 34.39 | 39.79[2] | 43.44[3] |
| Symbol rate [MBd] | 400 | 500 | 750 |

**TABLE 4.** G/S link budget parameters.

| Parameter | K-band 6.8 m | Q-band 3 m | Q-band 6.8 m | Q-band 10 m |
|---|---|---|---|---|
| Tracking loss [dB] | 0.19 | 0.19 | 1 | 2.16 |
| Antenna gain [dBi] | 61 | 61 | 69 | 72 |
| LNA[4] noise temperature [K] | 150 | 204.76 | | |

As expected, better performances (higher data returns) are obtained for:

- Locations at higher latitudes, due to the better contact time and climatic conditions (e.g. Svalbard vs. Graz)
- S/C and G/S with higher EIRP and gain respectively (e.g. 300 vs 50 kg satellite and 3 vs. 10 m antenna)
- Dynamic and adaptive transmission types (e.g. ACM vs. CCM)

Additionally, the results show that, under the same assumptions, the higher the orbit, the higher the data return. This is rather counter-intuitive, since the higher orbits are affected by a worse link budget (higher FSL), and reveals the clear impact of the increase in visibility.

In Table 5, the ''Performance comparison'' column shows the change with respect to the baseline scenario (#1) in terms of data (%) received per year. This comparison is done only among scenarios of the same satellite class (i.e. 300 kg)

In the case of Graz, despite being a limited location for EO data downlink due to the reduced contact time, the current study could benefit from the use of propagation measurements collected during the Alphasat (GEO) campaign at Q band [6]. The data collected at 35° elevation were extrapolated to different elevation angles using the cosecant law [12]. Fig. 5 shows the obtained results compared with the ITU-R P. 618-13 model predictions. As expected, the measurements match the model better at the measured elevation angle.

In scenario 16, these results are used for the computation of seasonal attenuation statistics and the evaluation of the performance of seasonal VCM. The better performing 8-sector VCM was considered for the analysis.

[2]Estimated phased array antenna size (with signal and power distribution) = 15 × 15 × 10 cm.

[3]Estimated parabolic reflector antenna size (including steering mechanism) = 20 × 20 × 20 cm.

[4]Low Noise Amplifier.

**TABLE 5.** Results of the end-to-end system performance analyses for 95% link availability for the different scenarios.

| Scenario | Orbit altitude [km] | S/C class [kg] | G/S antenna diameter [m] | Location | TX type | Comment | Data RX per pass [GB] | Obtained data availability [%] | Perform. Comparison [%] |
|---|---|---|---|---|---|---|---|---|---|
| **0** | 693 | >300 | 6.8 | Svalbard | CCM | K-band scenario Min. elev. = 11º | 119 | 99.5 | -56.2 |
| **1** | 693 | >300 | 6.8 | Svalbard | CCM | Baseline scenario Min. elev. = 11º | 272 | 99.4 | |
| **2** | 514 | >300 | 6.8 | Svalbard | CCM | Min. elev. = 8º | 232 | 99.6 | -13 |
| **3** | 824 | >300 | 6.8 | Svalbard | CCM | Min. elev. = 10º | 296 | 99.5 | +17.9 |
| **4** | 693 | <50 | 6.8 | Svalbard | CCM | Min. elev. = 10º | 170 | 99.6 | |
| **5** | 693 | >300 | 3 | Svalbard | CCM | Min. elev. = 15º | 206 | 99.4 | -31.1 |
| **6** | 693 | >300 | 10 | Svalbard | CCM | Min. elev. = 11º | 291 | 99.4 | +6.1 |
| **7** | 693 | >300 | 6.8 | Kiruna | CCM | Min. elev. = 11º | 240 | 99 | -24.4 |
| **8** | 693 | >300 | 6.8 | Sodankylä | CCM | Min. elev. = 8º | 232 | 99 | -25 |
| **9** | 693 | >300 | 6.8 | Graz | CCM | Min. elev. = 10º | 208 | 98.5 | -69.8 |
| **10** | 693 | >300 | 6.8 | Svalbard | VCM | 4 sectors | 321 | 99.2 | +50.4 |
| **11** | 693 | >300 | 6.8 | Svalbard | VCM | 8 sectors | 331 | 98.7 | +55.2 |
| **12** | 693 | <50 | 6.8 | Svalbard | VCM | 4 sectors | 205 | 99.2 | |
| **13** | 693 | <50 | 6.8 | Svalbard | VCM | 8 sectors | 211 | 99.2 | |
| **14** | 693 | >300 | 6.8 | Svalbard | ACM | | 369 | 100 | +90.3 |
| **15** | 693 | >300 | 6.8 | Graz | VCM | 8 sectors | 262 | 97.5 | -53.3 |
| **16** | 693 | >300 | 6.8 | Graz | Seasonal VCM | 8 sectors | 268 | 98.7 | -52.2 |

In Table 5, the obtained data availability (not to be confused with the link availability) is the ratio of transmitted to expected amount of received data.

## IV. CONCLUSION

The advantages of Q band (40 GHz) with respect to lower frequency bands (X band: 8 GHz, K band: 26 GHz) include larger available bandwidths (3 GHz in Q instead of 1.5 GHz in K), smaller antenna sizes for the same antenna gain and less interference from existing systems. On the other hand, the atmospheric losses and atmospheric noise collected by the G/S due to gases, clouds and mainly rain are much more severe at these frequencies. This is even more relevant in the case of non-geostationary Earth orbits, where the S/C spends most of the time at low elevation angles and even small fluctuations of atmospheric components can reduce the link availability.

Higher latitudes experience lower atmospheric absorption due to their climatic characteristics (i.e. colder and drier air). Low latitudes suffer from humid weather conditions and related higher propagation impairments, which become critical when tracking LEO satellites at low elevation angles: 10.4 dB increase in total attenuation exceeded at 99.5 % availability between Svalbard and Graz (Table 2).

Fade mitigation techniques (FMT) such as VCM and ACM enable in Svalbard, in comparison with CCM, data-volume return improvements of 55.2 % and 90.3 % respectively (Table 5).

Higher orbits yield higher data returns due to the increase in visibility: improvement of 13 % and 17.9 % when moving from 500 to 700 and then to 800 km orbit respectively with CCM in Svalbard (Table 5).

The current propagation models present limitations in their applicability to LEO orbits. Reliable propagation models need to cover all elevation angles, all seasons and dynamic characteristics (atmospheric and orbit dynamics) of LEO systems. The problem of the calculation of the tropospheric effects on low elevation links has become relevant recently.

It is necessary to foresee LEO propagation campaigns worldwide to develop adequate models at low elevations. Therefore, a possible follow-on propagation campaign would serve to improve the propagation prediction models and provide more accurate system design figures.

Finally, one of the key issues for further developing the Q band for EESS is its status as secondary service, a topic that is not analyzed in this contribution.

## ACKNOWLEDGMENT

This work was supported by the European Space Agency (ESA) under Contract 4000129101/20/NL/CT: "Feasibility Study of Q-Band (40 GHz) Earth Observation (EO) Data Downlink Systems," through the Austrian Research Promotion Agency. The views of the authors do not reflect the view of ESA.

## REFERENCES

[1] *Earth Exploration Satellite Service Handbook*, The International Telecommunication Union, Radio Communication Sector (ITU-R) Geneva, Switzerland, 2011.

[2] J. Rosello, A. Martellucci, R. Acosta, J. Nessel, L. E. Braten, and C. Riva, "26-GHz data downlink for LEO satellites," in *Proc. 6th Eur. Conf. Antennas Propag. (EUCAP)*, Mar. 2012, pp. 111–115.
[3] M. Jefferies, K. Maynard, P. Garner, J. Mayock, and P. Deshpande, "26-GHz data downlink and RF beacon for LEO in orbit demonstrator satellite," in *Proc. Int. Workshop Tracking, Telemetry Command Syst. Space Appl. (TTC)*, Sep. 2016, pp. 1–5.
[4] *Current and Future EUMETSAT Meteorological Satellite Networks, 'Second ITU/WMO Seminar Use of Radio Spectrum for Meteorology: Weather, Water and Climate Monitoring and Prediction*, Markus Dreis (EUMETSAT), Geneva, Switzerland, Oct. 2017.
[5] S. Ventouras, R. Reeves, and E. Rumi, "Large scale assessment of Ka/Q band atmospheric channel across Europe with ALPHASAT TDP5: The augmented network," in *Proc. 11th Eur. Conf. Antennas Propag. (EUCAP)*, Mar. 2017, pp. 1471–1475. [Online]. Available: https://ieeexplore.ieee.org/document/7928299
[6] F. Cuervo, A. Martellucci, J. Rivera Castro, M. Schmidt, and M. Schönhuber, "The alphasat Aldo Paraboni scientific and communication experiments at Ka and Q/V bands in Austria," *Int. J. Satell. Commun. Netw.*, vol. 37, no. 5, pp. 437–448, Sep. 2019, doi: 10.1002/sat.1308.
[7] *Propagation Data and Prediction Methods Required for the Design of Earthspace Telecommunication Systems*, document ITU-R Recommendation P.618-13, 2017.
[8] F. Cuervo, A. Martín-Polegre, F. Las-Heras, D. Vanhoenacker-Janvier, J. Flávio, and M. Schmidt, "Preparation of a CubeSat LEO radio wave propagation campaign at Q and W bands," *Int. J. Satell. Commun. Netw.*, to be published, doi: 10.1002/sat.1348.
[9] F. Cuervo, A. M. Polegre, D. Vanhoenacker-Janvier, J. Flavio, and M. Schmidt, "The Q/W-band cubesat LEO propagation experiment," in *Proc. 15th Eur. Conf. Antennas Propag. (EuCAP)*, Mar. 2021, pp. 1–5, doi: 10.23919/EuCAP51087.2021.9411255.
[10] N. Toptsidis, P.-D. Arapoglou, and M. Bertinelli, "Link adaptation for Ka band low Earth orbit earth observation systems: A realistic performance assessment," *Int. J. Satellite Commun. Netw.*, vol. 30, pp. 131–146, May/Jun. 2012.
[11] *Flexible Advanced Coding and Modulation Scheme for High Rate Telemetry, Applications*, document CCSDS 131.2-B-1, Mar. 2012.
[12] L. J. Ippolito, *Radiowave Propagation in Satellite Communications*. Dordrecht, The Netherlands: Springer, 2012, doi: 10.1007/978-94-011-7027-7.

**FELIX CUERVO** received the Diploma degree in telecommunication engineering from the University of Cantabria, Spain, in 2013, and the Ph.D. degree in information and communication technologies from the University of Oviedo, Spain, in 2021. He worked with the Space and Communications Technology Group, JOANNEUM RESEARCH, Graz, Austria, in propagation channel modeling for earth-space communication systems. He was part of the working groups, such as ASAPE and ITU-R Study Group 3.

**JOHANNES EBERT** received the master's and Ph.D. degrees in telematics from the Graz University of Technology, in 1995 and 2005, respectively. Since 1998, he has been working at JOANNEUM RESEARCH. He is the System Architect of the ground station in Graz and of the Alphasat Aldo Paraboni communication experiments. His research interests include satellite communication systems and signal processing.

**MICHAEL SCHMIDT** (Member, IEEE) received the master's degree in electrical engineering from the Graz University of Technology, Graz, Austria, in 1993. From 1993 to 1995, he worked at the Rutherford Appleton Laboratories, U.K., and Buckingham University, U.K., on the design of broadband communication systems. Since 1996, he has been with JOANNEUM RESAERCH, Graz, working in the fields of satellite communication with a focus on hardware and system design and the project management for ESA and EU projects. He is the Co-Principal Investigator (PI) in the Alphasat Aldo Paraboni communication experiments.

**PANTELIS-DANIEL ARAPOGLOU** (Member, IEEE) received the Diploma degree in electrical and computer engineering and the Dr.Eng. degree from the National Technical University of Athens (NTUA), Athens, Greece, in 2003 and 2007, respectively. From 2008 to 2010, he was involved in a postdoctoral research on MIMO over satellite jointly supported by the NTUA and the European Space Agency Research and Technology Centre (ESA/ESTEC), Noordwijk, The Netherlands. From 2010 to 2011, he was a Research Associate with the Interdisciplinary Centre for Security, Reliability and Trust (SnT), University of Luxembourg, Luxembourg, Luxembourg. Since 2011, he has been a Communications System Engineer with ESA/ESTEC, where he is technically supporting research and development activities and developments in the areas of satellite telecommunications, digital and optical communications, and high-data-rate telemetry for Earth observation applications.